

CrystEngComm

Accepted Manuscript

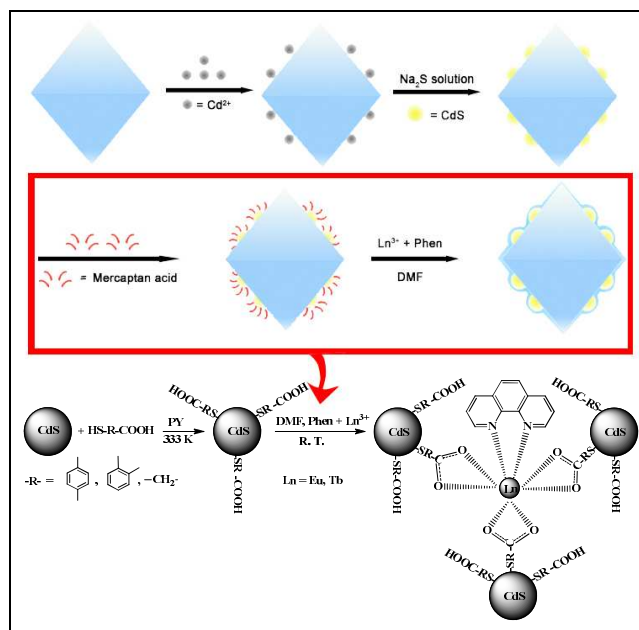


This is an *Accepted Manuscript*, which has been through the Royal Society of Chemistry peer review process and has been accepted for publication.

Accepted Manuscripts are published online shortly after acceptance, before technical editing, formatting and proof reading. Using this free service, authors can make their results available to the community, in citable form, before we publish the edited article. We will replace this *Accepted Manuscript* with the edited and formatted *Advance Article* as soon as it is available.

You can find more information about *Accepted Manuscripts* in the [Information for Authors](#).

Please note that technical editing may introduce minor changes to the text and/or graphics, which may alter content. The journal's standard [Terms & Conditions](#) and the [Ethical guidelines](#) still apply. In no event shall the Royal Society of Chemistry be held responsible for any errors or omissions in this *Accepted Manuscript* or any consequences arising from the use of any information it contains.



Novel luminescent hybrids are assembled by incorporating rare earth (Eu, Tb), mercaptan acid and 1,10-phenanthroline ternary complexes into CdS loaded zeolite Y through coordination reaction.

ARTICLE

Novel luminescent hybrids by incorporating rare earth ternary complex into CdS QDs loaded zeolite Y crystals through coordination reaction

Cite this: DOI: 10.1039/x0xx00000x

Tian-Wei Duan and Bing Yan*

Received 00th January 2012,
Accepted 00th January 2012

DOI: 10.1039/x0xx00000x

www.rsc.org/

A novel type of organic–inorganic zeolite-based hybrid material with excellent luminescence properties was synthesized. Firstly, we synthesized CdS QDs loaded zeolite crystals as hybrid matrix through ethanol solution reaction of sulfide ions and cadmium exchanged zeolite crystals. After that, we functionalized CdS QDs loaded zeolite with three different mercaptan acid, thiosalicylic acid (*o*-MBA), 4-mercatobenzoic acid (*p*-MBA), and mercaptoacetic acid (MAA), respectively, and then the mercaptan acid modified CdS QDs loaded zeolite and 1,10-phenanthroline was applied to coordinate with rare earth (Eu³⁺, Tb³⁺). Accordingly, the final hybrid materials were formed by a mild coordination reaction. Fluorescent spectra were used to investigate the photophysical properties of hybrid materials, which indicate the emission spectra of obtained hybrid materials varies due to the different match degree between triplet energy level of all three mercaptan acid and excited energy level of rare earth (Eu³⁺, Tb³⁺). Besides, findings also reveal that the photoluminescence color can be tuned from white, pink to red by changing the coordination mercaptan acid. Among the obtained materials, the europium, mercaptoacetic acid (MAA) and 1,10-phenanthroline ternary complexes functionalized CdS-ZY show remarkable luminescence quantum yields and relatively long ⁵D₀ lifetimes at room temperature.

Introduction

Luminescence lanthanide compounds have been paid much attention thanks to attractive features of high color purity, high luminescence quantum efficiencies, and a wide range of lifetimes. These photoluminescence properties have attracted much attention for a variety of potential applications, such as light emitting devices, luminescent probes, and optical imaging¹. However, the practical application of lanthanide compounds is hindered by their poor physical stability and low mechanical strength. In order to overcome these drawbacks, the solution is to immobilize the lanthanide compounds in stable matrices, like polymers², ionic liquid^{3, 4}, silicon materials⁵, etc. In the past decades, microporous materials used as a support for lanthanide compounds have attracted much attention⁶. In the field of inorganic microporous materials, zeolites crystals are widely used because of the distinctive framework structure. Zeolites are microporous crystalline aluminosilicates, whose general formula corresponds to Mⁿ⁺_{x/n}[(AlO₂)_x(SiO₂)_y]·mH₂O. The channels and pores of zeolite are formed by a three-directional network of [AlO₄]⁵⁻ and [SiO₄]⁴⁻ tetrahedra linked via bridging oxygen atoms⁷. As for the new insight into zeolite, the rigid structure of framework and the reducing environment of cavities have opened new possibilities for synthesis novel host-guest luminescence materials. For nearly a decade, a variety of luminescence source are cooperated into zeolite pores. However, the confined pore size of zeolite limits embedded guest species, which possess small sizes including metal ions⁸, lanthanide compounds⁹, metal ion clusters¹⁰,

and semiconductor clusters¹¹. There are many routes for incorporating luminescence center into zeolite crystals, such as ion exchange, vapor impregnation, solid-state diffusion, ship-in-bottle synthesis^{12, 13}. Sometimes, more than one method is used to synthesis luminescent zeolite materials in order to get outstanding luminescence performance. Ion exchange method should be the conventional process to modify zeolite crystals. Because zeolite has many cages and channels, cations are free to migrate in and out zeolite structures. The ability of ion exchange is defined by ion exchange degree of zeolite crystals, which varies because of different zeolite topologies and diverse combination between exchanged ions and skeleton atoms. Metal clusters loaded zeolite crystal has been a hot area of research for several years. In recent years, a variety of metal clusters loaded zeolite with specific luminescence properties are designed by scientist^{14, 15}. Eduardo and co-workers^{16a} have measured the external quantum efficiency (EQE) of silver-clusters zeolite composites, which have EQEs up to 69 %. Because of the large Stokes shift and high EQE, these materials could be potentially used as phosphors for the fabrication of fluorescent lamps and as wavelength convertors in solar cells. Sun and coworkers^{16b} have synthesized a bismuth-embedded zeolite Y crystal yields luminescent Bi³⁺ without the formation of metallic nanoparticles through thermal treatment and it suggest that all Bi³⁺ are optically active in the near-infrared (NIR) spectral range and the emission line shapes under diverse excitation wavelengths greatly depend on the Bi concentration and annealing temperature.

Our group has done several studies on the synthesis and

photoluminescence properties studies of lanthanide complexes covalently bonded to porous materials. It is shown that promising visible-luminescent properties can be obtained by linking the lanthanide complexes to porous materials¹⁷. Attractive properties of rare-earth based semiconductor nanoparticles include high photostability, narrow emission lines and long lifetimes that can be exploited for detection schemes, and mild functionalization strategies^{18a}. Rare earth and CdS hybrid materials have shown some novel photophysical properties, for example, an enhanced fluorescence from Eu³⁺ doped silica gels in which CdS nanoparticles were adsorbed onto the pore surface of the gels is observed^{18b}. Our group has investigated into 3-mercaptopropyltrimethoxysilane (MPS) functionalized MPS-CdS nanocomposite and obtained remarkable quantum yield^{18c}. Inspired by the above discussion, we have incorporated some rare earth (Eu³⁺, Tb³⁺) ternary complexes into cadmium sulfide loaded zeolite crystals through the coordination reaction. Zeolite Y crystals with high ion exchange degree is used here as the matrix materials. Cadmium ion exchanged zeolite crystals are firstly converted to cadmium sulfide loaded zeolite by introduction of sulfur source in ethanol solution reaction. Then cadmium sulfide loaded zeolite Y crystals is modified with mercaptan acid (thiosalicylic acid (*o*-MBA), 4-mercatobenzoic acid (*p*-MBA), mercaptoacetic acid (MAA)) to form organic-inorganic molecular bridge. After that, the rare earth ions and 1,10-phenanthroline are introduced into mercaptan acid modified cadmium sulfide loaded zeolite Y crystals using a mild coordination reaction. Consequently, a series of ternary rare earth complexes functionalized cadmium sulfide loaded zeolite crystal are prepared and characterized. To the best of our knowledge, this is the first time that the rare earth luminophores are incorporated into cadmium sulfide loaded zeolite crystals by means of the coordination reaction. The approach presented in this work is a general one and can be extended to construct other kinds of functional QDs loaded crystalline materials.

Experimental Section

Materials

NaY zeolite crystal was synthesis by using NaAlO₂, Ludox HS-40 and NaOH. EuCl₃·6H₂O and TbCl₃·6H₂O were prepared by dissolving their corresponding oxides in concentrated hydrochloric acid followed by evaporation. Cadmium acetate (98.5 %, Cd(CH₃COO)₂·2H₂O), sodium sulfide (98 %, Na₂S·9H₂O), thiosalicylic acid (98 %, *o*-MBA), 4-mercatobenzoic acid (98 %, *p*-MBA), mercaptoacetic acid (GR, MAA), 1,10-phenanthroline monohydrate (99 %), pyridine (AR, PY) and cyclohexane (AR, CYH) were purchased from reagent company and used as received.

Preparation of CdS-ZY composites

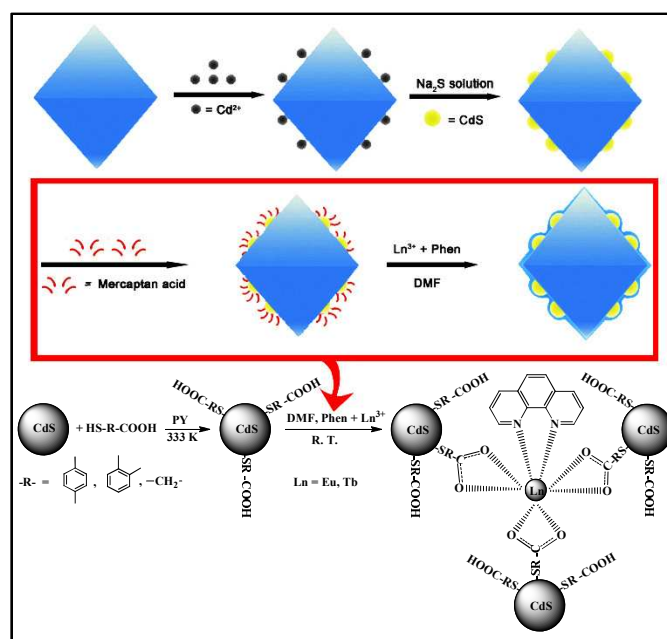
Zeolite Y crystals was produced by following the procedure reported in literature^{19a}. The procedure of synthesis zeolite Y crystal was as follows: 2.337 g NaAlO₂ was added into 8 mL 1.25 mol·L⁻¹ NaOH and stirred for an hour. 9.845 g Ludox HS-4015 was dissolved in 3.62 mL distilled water and was stirred for an hour. While stirring, silica solution was slowly added into the first solution and continued stirring for 5 hrs. At this time the solution was sealed in bombs and left at room temperature for 48 hrs and then at 373 K for 12 hrs. Obtained NaY zeolite were washed till pH = 7 with distilled water and were dried in the air thoroughly at 373 K overnight. The following procedure was the preparation of CdS-Zeolite Y 1.0 g zeolite Y was added to a 50 mL solution of ethanol containing 0.01 M cadmium acetate. The covered solution was stirred for 48 hrs. Obtained Cd²⁺ exchanged zeolite Y was washed by ethanol to get rid of redundant Cd²⁺ ions. A 50 mL solution of

ethanol containing 0.01 M sodium sulfide was prepared and slowly added into the cadmium acetate solution while stirring, resulting in a yellow colored precipitate. The resulting solution was covered and stirred for 24 hrs. The precipitate was then removed from solution by centrifugation, washed several times with ethanol, and dried overnight in a vacuum oven at 373 K. The obtained CdS-Zeolite Y crystal is kept in drier. We denote the CdS-Zeolite Y composites as CdS-ZY.

Preparation of mercaptan acid modified CdS-ZY

Three different mercaptan acid, *o*-MBA, *p*-MBA and MAA, were applied to modify CdS-ZY. A typical procedure for the preparation of *o*-MBA (or *p*-MBA) modified CdS-ZY was as follows: 100 mg CdS-ZY and 0.1 mmol (0.01542 g) *o*-MBA (or *p*-MBA) was added in 20 mL of pyridine. The mixture was heated at 333 K in a covered flask for approximately 3 hrs with stirring. Pyridine can be removed by rotary evaporation. *o*-MBA (or *p*-MBA) modified CdS-ZY was obtained by washed with cyclohexane. The product was dried in vacuum at 333 K. The procedure for synthesis of MAA modified CdS-ZY is to add 100 mg CdS-ZY and 0.1 mmol (about 0.01 mL) MAA in 20 mL ethanol, and followed by centrifugation and dried in a vacuum oven at 333 K. We denote the obtained materials as (*o*-MBA)-CdS-ZY, (*p*-MBA)-CdS-ZY and (MAA)-CdS-ZY.

Preparation of rare earth complexes functionalized CdS-ZY



Scheme 1 Illustration of the synthesis procedure of rare earth complexes functionalized CdS-ZY and predicted structure of the lanthanide ternary complex functionalized CdS-ZY hybrid materials.

The rare earth and 1,10-phenanthroline were introduced into mercaptan acid modified CdS-ZY using a mild coordination reaction. The precursors 0.033 mmol (0.0121 g) EuCl₃·6H₂O (or 0.0123 g TbCl₃·6H₂O) and 0.033 mmol (0.0065 g) phenanthroline (phen) monohydrate are dissolved in DMF (15 mL) solvent with stirring for 15 min. Powder CdS-ZY was dispersed in the as-prepared rare earth complex DMF solution by stirring. Then the mixture was under vigorous stirring at room temperature. After reaction for 6 hrs, the hybrid zeolite material was collected by centrifugation, washed several times with ethanol and dried overnight in vacuum oven at 333 K for characterization. The hybrid materials are kept in drier. We denote the obtained hybrid materials as Eu(phen)(*o*-MBA)₃-CdS-ZY, Tb(phen)(*o*-MBA)₃-CdS-ZY, Eu(phen)(*p*-MBA)₃-

CdS-ZY, Tb(phen)(*p*-MBA)₃-CdS-ZY, Eu(phen)(MAA)₃-CdS-ZY, and Tb(phen)(MAA)₃-CdS-ZY. (See Scheme 1)

Physical characterization

Infrared spectra were measured within KBr pellets from 4000 to 400 cm⁻¹ using a Nexus 912 AO446 Fourier transform infrared spectrum radiometer (FTIR). X-ray powder diffraction patterns (XRD) were acquired on Rigaku D/max-rB diffractometer equipped with Cu anode; the data were collected within the 2θ range of 5-65°. Energy Dispersive Analysis by X-rays (EDAX) and transmission electron microscope (TEM) is carried out on a JEOL JEM-2010F electron microscope operated at 200 kV. Thermogravimetric analysis (TG) was measured using a Netzsch STA 449C system at a heating rate of 5 °C/min under the nitrogen protection. The diffuse reflectance UV diffusion reflection spectra of the powdered samples were recorded by a B&WTEK BWS003 spectrophotometer. Luminescence excitation spectra and emission spectra were measured on an Edinburgh FLS920 fluorescence spectrometer. The lifetime and efficiencies measurements were measured on an Edinburgh Instruments FLS 920 fluorescence spectrometer.

Results and discussion

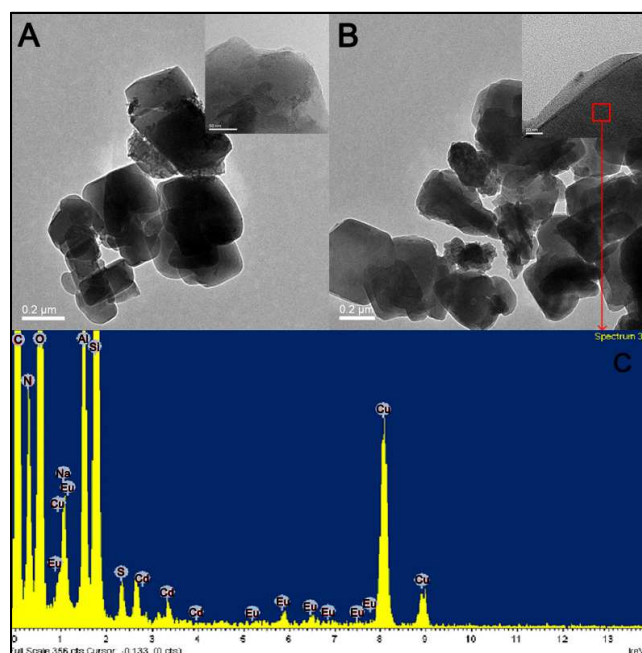


Figure 1 (A) TEM image of the CdS-ZY. (B) TEM image of the Eu(phen)(*o*-MBA)₃-CdS-ZY. (C) EDXA analysis of the Eu(phen)(*o*-MBA)₃-CdS-ZY.

A series of CdS-ZY hybrid materials were prepared via a mild coordination reaction. The synthesis procedure and the predicted structure of this hybrid are shown in Scheme 1. In the first step, the synthesized zeolite Y crystal was loaded with cadmium ions through ion exchange process. Subsequently, an ethanol solution of sodium sulfide was used to react with cadmium ions loaded zeolite. In the meanwhile, the CdS-zeolite Y composite was formed. However, CdS QDs are not only in the pores of zeolite but also on the surface of zeolite crystal. It can be proved by TEM images (Figure 1). In the next step, three different mercaptan acid were performed separately on the CdS-ZY composite to modify CdS QDs. Then an coordination reaction was performed among mercaptan acid modified CdS-ZY, phen, and rare earth ions, producing rare earth complexes functionalized CdS-ZY. It proved to be difficult to get the exact

structure of this kind of hybrid material and it is hardly to solve the coordination behavior of lanthanide ions. The main composition, lanthanide coordination principle and the configuration of the organic functional groups, however, are knowable. The rare earth trivalent ions are hard Lewis acids so they readily coordinate with hard bases containing oxygen and nitrogen atoms. Additionally, most of the lanthanide complexes hold polar covalent bonds as the lanthanide ions always bond through the 6s, 6p, and 5d electronic orbitals, whose electron count is nine. Therefore, it is most stable for the lanthanide complex to exist with the coordination number of eight or nine. Furthermore, in our experiment we synthesize the material by adding the appropriate and accurate proportion of reagent into the system to obtain the fixed model of lanthanide complex. Furthermore, in view of the spatial steric hindrance effect, we predicted the optimum coordination structure for the hybrid material.

Figure 1 shows the selected transmission electron microscopy (TEM) images of CdS-ZY and Eu(phen)(*o*-MBA)₃-CdS-ZY, including EDXA analysis of the Eu(phen)(*o*-MBA)₃-CdS-ZY. Minority of CdS QDs were formed inside the pores of zeolite Y. The aggregation of CdS QDs exists on the external surface of zeolite since a small amount of Cd²⁺ ions cling to the zeolite surface during performing introduction of sulfur ions. Meanwhile, due to the functionalization is simple and relatively mild, the microstructure of zeolite can be substantially conserved after the introduction of rare earth complex units through coordination reaction, which has also been confirmed by the XRD patterns before and after functionalization (Figure S1). A thin film of rare earth complex was formed and enclosed zeolite after coordination reaction. It is probably because the modified mercaptan acid are mainly on the surface of zeolite when reaction with 1,10-phenanthroline and rare earth ions as shown in scheme 1.

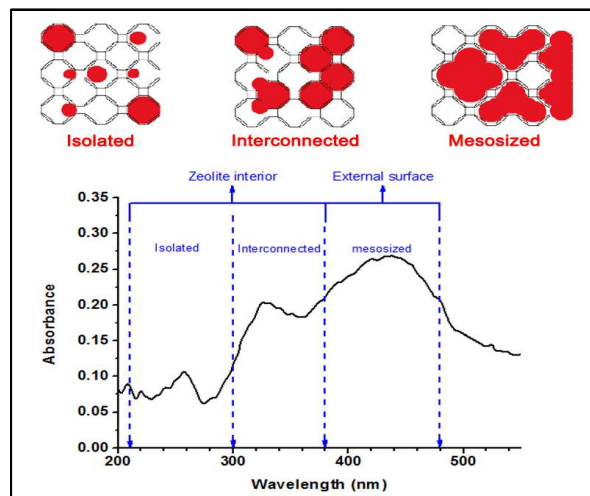


Figure 2 Uv-vis diffusion reflection spectra of CdS-ZY and three type of the distribution of CdS QDs intra zeolite.

The distribution of CdS QDs can be confirmed by the Uv-vis diffusion reflection spectra. According to literature^{19b}, in the case of CdS QDs, the absorption maxima wavelength of the isolated QDs, interconnected QDs, and mesosized QDs appear in the 200-300 nm, 300-380 nm, and 380-480 nm regions, respectively. Therefore, it can be predicted from Uv-vis reflection spectra that intrazeolite CdS QDs exist in zeolite Y crystals in three types, isolated, interconnected, and mesosized (Figure 2). The domination existence form of intrazeolite CdS QDs is in mesosized type. The transmission electron microscopy (TEM) image of the framework of CdS-ZY was partially destroyed and mesosized CdS QDs exist mostly on the

external surface (Figure S2). Fortunately, it can be proved by comparing the XRD pattern of CdS-ZY and zeolite Y crystals (Figure S3). The intensity of (1,1,1) crystal plane, which is included in β supercell of zeolite Y crystal, is relatively lower in CdS-ZY than zeolite Y crystal. It is mainly because the aggregation of the isolated CdS QDs accompanies a large degree of framework destruction, which leads to inevitable damage on (1,1,1) crystal plane.

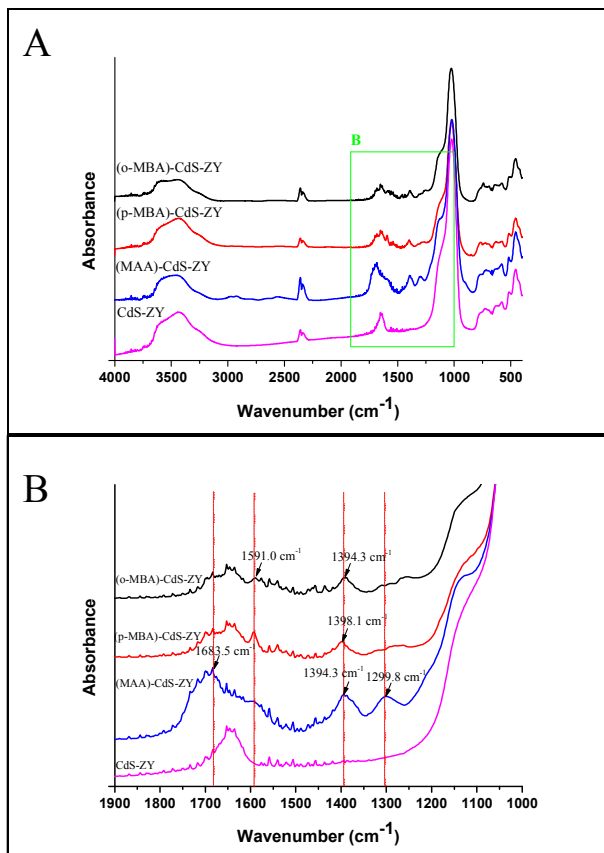


Figure 3 FTIR spectra of three different mercaptan acid modified CdS-ZY and spectra of pure CdS-ZY ranged from 400 ~ 4000 cm^{-1} (A) and ranged from 1000 ~ 1900 cm^{-1} .

Figure 3 shows the FTIR spectra of mercaptan acid modified CdS-ZY and CdS-ZY. Because the functionalization of CdS-ZY is partial, the amount of mercaptan acid is so low that the intensity of peaks related to vibrational frequencies of the group are hardly observed. The characteristic adsorption bands of mercaptan acid can only be observed from zoomed spectra (Figure 3B). The stretching vibration of S-H is around 2560 cm^{-1} , however, this absorbance peak is not showed in the spectra of three different mercaptan modified CdS-ZY. It predicts that sulfhydryl group is successfully coordinating with cadmium ions. The asymmetrical vibration of C=O is about 1683 cm^{-1} , and peaks centered at this vibration frequencies can be observed in three mercaptan acid FTIR spectra. As for thiosalicylic acid or 4-mercatobenzoic acid modified CdS-ZY, the skeletal vibration of benzene around 1591 cm^{-1} is showed in both spectra. The peak centered at 1394 cm^{-1} and 1299 cm^{-1} are separately attributed to the vibration of $\text{CH}_2\text{-S}$ ($-\text{CH-S}$) and the vibration of C-O. The successful attachment of rare earth complex unit to the polymer backbones is supported by the disappearance of asymmetrical vibration of C=O centered at 1683 cm^{-1} and vibration of C-O around 1299 cm^{-1} . Moreover, it can be observed that the vibration of the symmetrical vibration

of two C=O links in the resonating structure of the coordinated mercaptan acid around 1594 cm^{-1} (Figure S4). Nevertheless, the presence of europium, sulfur, oxygen and nitrogen in the EDAX spectrum (Figure 1C) provide a positive evidence for the successful functionalization to CdS-ZY.

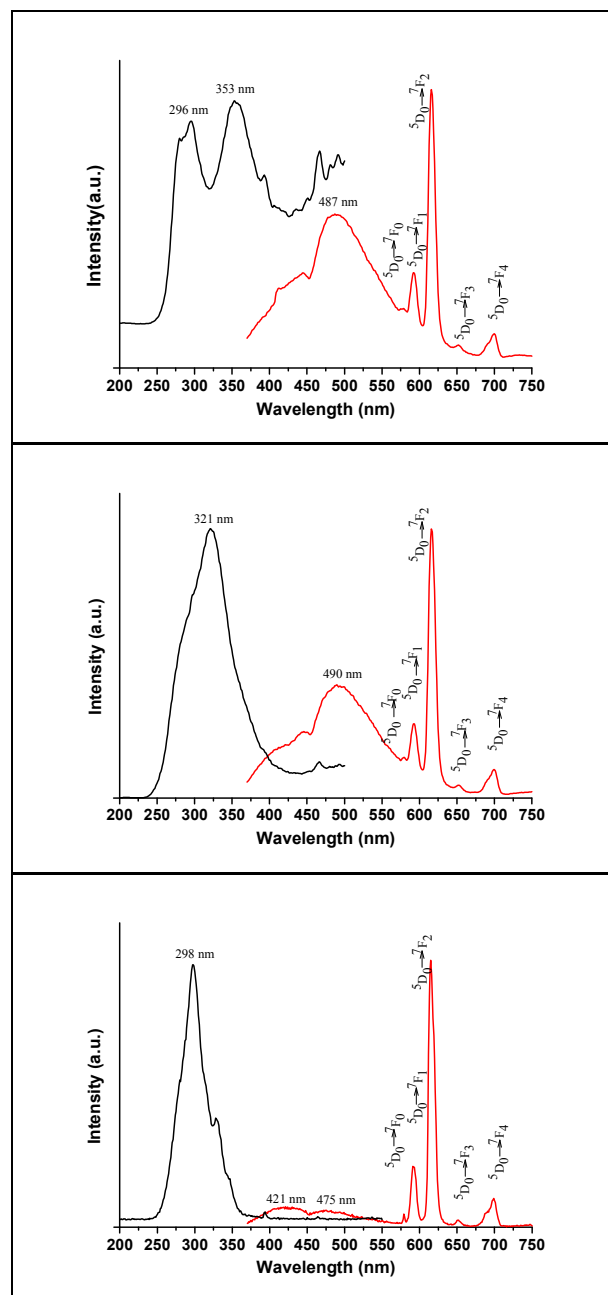


Figure 4 Excitation and emission spectrum of $\text{Eu}(\text{phen})(o\text{-MBA})_3\text{-CdS-ZY}$, $\text{Eu}(\text{phen})(p\text{-MBA})_3\text{-CdS-ZY}$ and $\text{Eu}(\text{phen})(\text{MAA})_3\text{-CdS-ZY}$. (A) $\text{Eu}(\text{phen})(o\text{-MBA})_3\text{-CdS-ZY}$ excitation spectrum is obtained by monitoring the emission of Eu^{3+} at 616 nm, and the excitation wavelength for the emission spectrum is 296 nm. (B) $\text{Eu}(\text{phen})(p\text{-MBA})_3\text{-CdS-ZY}$ excitation spectrum is obtained by monitoring the emission of Eu^{3+} at 616 nm, and the excitation wavelength for the emission spectrum is 321 nm. (C) $\text{Eu}(\text{phen})(\text{MAA})_3\text{-CdS-ZY}$ excitation spectrum is obtained by monitoring the emission of Eu^{3+} at 616 nm, and the excitation wavelength for the emission spectrum is 298 nm.

The excitation spectra for europium complexes functionalized CdS-ZY were obtained by monitoring the characteristic emission of europium ion at 616 nm and were presented on the left Figure 4. It is

clearly from the figures that all the excitation spectra dominated by a broad absorption bands located at ultraviolet region, suggesting that the resulted materials can absorb the ultraviolet light efficiently and then sensitize the emission of europium ion by energy transfer. Furthermore, the maxima excitation wavelength of the functionalized CdS-ZY at about 296, 321 and 298 nm for Eu(phen)(*o*-MBA)₃-CdS-ZY, Eu(phen)(*p*-MBA)₃-CdS-ZY and Eu(phen)(MAA)₃-CdS-ZY, respectively, which is mainly attributed to the different singlet state energy levels of $\pi \rightarrow \pi^*$ transition taken place in mercaptan acid under excitation of ultraviolet lights. Here the emission spectra are obtained by using the most appropriate wavelength described above as the excitation wavelength and presented on the right of the Figure 4. The emission band of europium complexes functionalized CdS-ZY contains a broad band ranging from 360 nm to 550 nm, caused by the emission of matrix. The matrix emission centered at 487, 490, 475 nm, for Eu(phen)(*o*-MBA)₃-CdS-ZY, Eu(phen)(*p*-MBA)₃-CdS-ZY and Eu(phen)(MAA)₃-CdS-ZY, respectively, are separately in accordance with the emission spectra of (*o*-MBA)-CdS-ZY, (*p*-MBA)-CdS-ZY and (MAA)-CdS-ZY (Figure S5). It is probably due to the fact that the defect in crystal lattice yields the contribution to the emission of zeolite matrix. In the excitation of [AlO₄]⁵⁻ and [SiO₄]⁴⁻, the hole (on oxygen) and the electron may remain together generating luminescence. Because of the emission of rare earth ions dominates the emission spectra of the resulted materials, hence, the europium complex functionalized CdS-ZY possess similar emission spectra originating from the characteristic transitions of europium ions. As shown in Figure 4, the emission lines are assigned to ⁵D₀→⁷F₀, ⁵D₀→⁷F₁, ⁵D₀→⁷F₂, ⁵D₀→⁷F₃ and ⁵D₀→⁷F₄ transitions for those peaks located at about 578, 592, 616, 652 and 700 nm, respectively. It can be observed that all the emission spectra shown in Figure 4A are dominated by a very intense ⁵D₀→⁷F₂ transition at about 616 nm. It is well known that the ⁵D₀→⁷F₂ transition is a typical electric dipole transition and is very sensitive to the local symmetry of europium ions⁴⁵, while the parity-allowed magnetic dipole transition ⁵D₀→⁷F₁ is practically independent of the ion's surroundings. Hence, the intensity ratios I(⁵D₀→⁷F₂)/I(⁵D₀→⁷F₁) (I₀₂/I₀₁) can be seen as an indicator for the local environment of ions. According to the intensity ratio listed in Table 1, we concluded that the chemical environment around the europium ions is in low symmetry.

As shown on the left of the Figure 5, the excitation spectra of terbium complexes functionalized CdS-ZY also exhibit a broad excitation band at ultraviolet region. It can be observed that the maximum excitation wavelength of the final materials at about 296, 321 and 298 nm for Tb(phen)(*o*-MBA)₃-CdS-ZY, Tb(phen)(*p*-MBA)₃-CdS-ZY and Tb(phen)(MAA)₃-CdS-ZY, respectively, which mainly consist with the absorption bands observed in the excitation spectra of europium functionalized CdS-ZY. It also can be observed the emission of matrix ranged from 360 ~ 550 nm in all the terbium complexes functionalized CdS-ZY. The emission lines of terbium complexes functionalized CdS-ZY depicted on the right of Figure 5 are assigned to ⁵D₄→⁷F₆, ⁵D₄→⁷F₅, ⁵D₄→⁷F₄ and ⁵D₄→⁷F₃ transitions located at 491, 545, 585 and 621 nm, respectively. The green fluorescence is observed for all the terbium complexes functionalized CdS-ZY mainly due to the fact that the ⁵D₄→⁷F₅ transition is the most intense one. Among all the terbium complexes functionalized CdS-ZY, MAA and 1,10-phenanthroline ternary complexes functionalized CdS-ZY shows higher matrix luminescence than other mercaptan acid modified CdS-ZY and it probably because the triplet energy level of MAA doesn't match well with excited energy level of Tb³⁺.

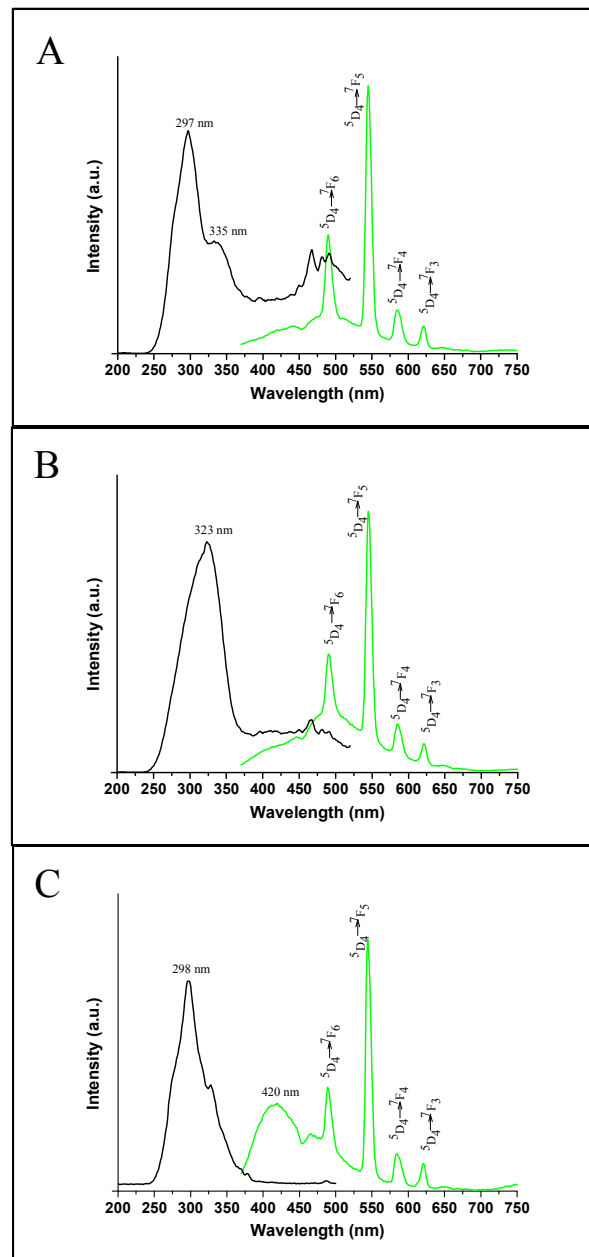


Figure 5 Excitation and emission spectrum of Tb(phen)(*o*-MBA)₃-CdS-ZY, Tb(phen)(*p*-MBA)₃-CdS-ZY and Tb(phen)(MAA)₃-CdS-ZY. (A) Tb(phen)(*o*-MBA)₃-CdS-ZY excitation spectrum is obtained by monitoring the emission of Tb³⁺ at 545 nm, and the excitation wavelength for the emission spectrum is 297 nm. (B) Tb(phen)(*p*-MBA)₃-CdS-ZY excitation spectrum is obtained by monitoring the emission of Tb³⁺ at 545 nm, and the excitation wavelength for the emission spectrum is 323 nm. (C) Tb(phen)(MAA)₃-CdS-ZY excitation spectrum is obtained by monitoring the emission of Tb³⁺ at 545 nm, and the excitation wavelength for the emission spectrum is 298 nm.

Interestingly, the photoluminescence color can be tuned from white, pink to red by changing the coordination mercaptan acid. Figure 6 shows the corresponding CIE chromaticity diagram of europium or terbium complexes functionalized CdS-ZY with different coordination mercaptan acid. The emission of europium or terbium complexes functionalized CdS-ZY is related to the energy matching of transition energy level of rare earth and triplet level of coordination molecule. The luminescence of europium complexes functionalized CdS-ZY with different mercaptan acid are significantly changed, which is probably caused by the different

energy transfer ability of coordination mercaptan acid. However, the luminescence change of terbium complexes functionalized CdS-ZY is less obvious than europium. The corresponding luminescence color can be seen clearly from the photographs of europium or terbium complexes functionalized CdS-ZY samples (Figure 6), where an appropriate wavelength was used as the excitation source.

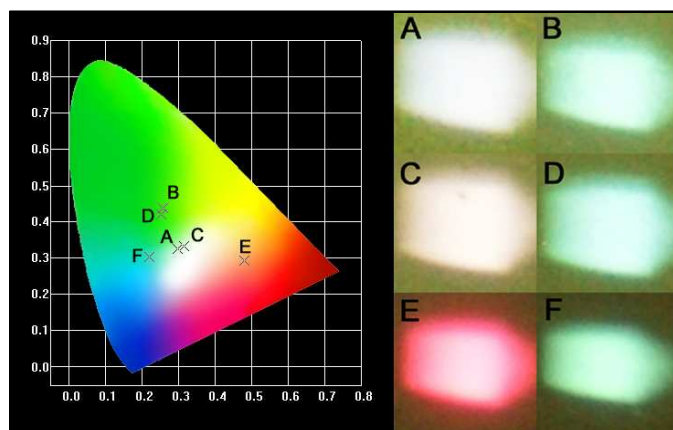


Figure 6 CIE x-y chromaticity diagram of hybrid materials. (A) Eu(phen)(*o*-MBA)₃-CdS-ZY ($\lambda_{\text{ex}} = 296$ nm) (B) Tb(phen)(*o*-MBA)₃-CdS-ZY ($\lambda_{\text{ex}} = 297$ nm) (C) Eu(phen)(*p*-MBA)₃-CdS-ZY ($\lambda_{\text{ex}} = 321$ nm) (D) Tb(phen)(*p*-MBA)₃-CdS-ZY ($\lambda_{\text{ex}} = 323$ nm) (E) Eu(phen)(MAA)₃-CdS-ZY ($\lambda_{\text{ex}} = 298$ nm) (F) Tb(phen)(MAA)₃-CdS-ZY ($\lambda_{\text{ex}} = 298$ nm).

For further investigation of the photoluminescence properties, we measure the luminescence lifetime decay curves of the lanthanide complexes functionalized CdS-ZY at room temperature, the resulting lifetimes are given in Table 1. For the europium complexes functionalized CdS-ZY, the luminescence lifetime decay curves of the europium $^5\text{D}_0 \rightarrow ^7\text{F}_2$ transition are found to a single exponential form, indicating that all europium ions locate in the same average environment. The typical decay curves of selected europium complexes functionalized CdS-ZY and their corresponding fitted curves are shown in Figure S5 as examples. Besides, we measure efficiencies on an Edinburgh Instruments FLS 920 fluorescence spectrometer and the resulting emission quantum efficiencies are listed in Table 1. As shown in the table, europium, mercaptoacetic acid (MAA) and 1,10-phenanthroline ternary complexes functionalized CdS-ZY has better quantum efficiency and longer luminescence lifetimes than other europium mercaptan acid complexes functionalized CdS-ZY for the materials derived from the same CdS-ZY matrix. As we known, the triplet state energy of 2-thenoyltrifluoroacetate (tta) matches very well with the excited energy of europium. Compared to $\text{Eu}^{3+}(\text{tta})_x(\text{phen})_y$ complex and zeolite L host-guest materials ($\text{Eu}^{3+}(\text{tta})_x(\text{phen})_y\text{-ZL}$)^{19c} ($\eta = 38\%$), the quantum efficiency of Eu(phen)(MAA)₃-CdS-ZY ($\eta = 16\%$) is little bit lower. But the luminescence lifetimes of Eu(phen)(MAA)₃-CdS-ZY ($\tau = 0.71$ ms) is equal to that of $\text{Eu}^{3+}(\text{tta})_x(\text{phen})_y\text{-ZL}$ ($\tau = 0.75$ ms).

Table 1 The luminescent efficiencies and lifetimes for the europium and terbium complexes functionalized CdS-ZY.

Materials	I_{02}/I_{01} ^a	τ (μs) ^b	η (%) ^c
Eu(phen)(<i>o</i> -MBA) ₃ -CdS-ZY	2.72	281.4	7.6
Eu(phen)(<i>p</i> -MBA) ₃ -CdS-ZY	3.22	262.3	1.6
Eu(phen)(MAA) ₃ -CdS-ZY	4.51	712.7	16
Tb(phen)(<i>o</i> -MBA) ₃ -CdS-ZY	--	527.2	4.9
Tb(phen)(<i>p</i> -MBA) ₃ -CdS-ZY	--	491.9	1.7
Tb(phen)(MAA) ₃ -CdS-ZY	--	363.6	11

^a The emission intensity ratios of the $^5\text{D}_0 \rightarrow ^7\text{F}_1$ transition (I_{01}) and the $^5\text{D}_0 \rightarrow ^7\text{F}_2$ transition (I_{02}) for europium functionalized CdS-ZY; ^b lifetimes (τ) of $^3\text{D}_0$ energy level and $^5\text{D}_4$ energy level for Eu^{3+} and Tb^{3+} excited state, respectively; ^c the luminescent quantum efficiencies are measured on an Edinburgh Instruments FLS 920 fluorescence spectrometer.

Conclusions

We have designed and synthesized a series of novel luminescent zeolite crystals by incorporating rare earth (Eu^{3+} , Tb^{3+}), mercaptan acid and 1,10-phenanthroline ternary complexes into CdS QDs loaded zeolite. Since the different match degree between triplet energy level of all the three mercaptan acid and excited energy level of rare earth (Eu^{3+} , Tb^{3+}), the photoluminescence color can be tuned by changing the coordination mercaptan acid. Results shows that the synthesis method reported here is an advisable one for constructing luminescent zeolite materials. The synthesis process may be applied to other systems and the final materials can be expected to a promising light-conversion material.

Acknowledgements

This work was supported by the National Natural Science Foundation of China (20971100, 91122003), Program for New Century Excellent Talents in University (NCET 2008-08-0398).

Notes and references

^a Department of Chemistry, Tongji University; State Key Lab of Water Pollution and Resource Reuse (Tongji University), Siping Road 1239, Shanghai 200092, China. Fax: +86-21-65982287; Tel: +86-21-65984663; E-mail: byan@tongji.edu.cn

[†] Footnotes should appear here. These might include comments relevant to but not central to the matter under discussion, limited experimental and spectral data, and crystallographic data.

Electronic Supplementary Information (ESI) available: [details of any supplementary information available should be included here]. See DOI: 10.1039/b000000x/

References

- (a) S. V. Eliseeva and J. C. G. Bunzli, *Chem. Soc. Rev.*, 2010, **39**, 189-227; (b) T. Matsuya, N. Hoshino and T. Okuyama, *Curr. Anal. Chem.*, 2006, **2**, 397-410; (c) S. Mizukami, T. Yamamoto, A. Yoshimura, S. Watanabe and K. Kikuchi, *Angew. Chem. Int. Edit.*, 2011, **50**, 8750-8752.
- (a) Y. F. Shao, B. Yan and Z. Y. Jiang, *Rsc. Adv.*, 2012, **2**, 9192-9200; (b) H. L. Tan, C. J. Ma, Y. H. Song, F. G. Xu, S. H. Chen and L. Wang, *Biosens. Bioelectron.*, 2013, **50**, 447-452.
- (a) P. S. Campbell, C. Lorbeer, J. Cybinska and A. V. Mudring, *Adv. Funct. Mater.*, 2013, **23**, 2924-2931; (b) Q. R. Ru, Y. G. Wang, W. J. Zhang, X. Y. Yu and H. R. Li, *Eur. J. Inorg. Chem.*, 2013, 2342-2349.
- (a) J. Cuan and B. Yan, *Dalton. T.*, 2013, **42**, 14230-14239; (b) Y. F. Shao, B. Yan and Q. P. Li, *Eur. J. Inorg. Chem.*, 2013, 381-387; (c) Q. P. Li and B. Yan, *Dalton. T.*, 2012, **41**, 8567-8574.
- (a) L. N. Sun, W. P. Mai, S. Dang, Y. N. Qiu, W. Deng, L. Y. Shi, W. Yan and H. J. Zhang, *J. Mater. Chem.*, 2012, **22**, 5121-5127; (b) B. Yan and Y. F. Shao, *Dalton. Trans.*, 2013, **42**, 9565-9573.
- (a) Y. Chen and S. Q. Ma, *Rev. Inorg. Chem.*, 2012, **32**, 81-100; (b) J. Rocha, L. D. Carlos, F. A. A. Paz and D. Ananias, *Chem. Soc. Rev.*, 2011,

- 40, 926-940; (c) B. Ay, E. Yildiz, J. D. Protasiewicz and A. L. Rheingold, *Inorg. Chim. Acta.*, 2013, **399**, 208-213.
7. S. L. Suib, *Science*, 2003, **302**, 1335-1336.
8. (a) J. A. Peters and K. Djanashvili, *Eur. J. Inorg. Chem.*, 2012, 1961-1974; (b) V. O. Vasylechko, G. V. Gryshchouk, V. P. Zakordonskiy, I. O. Patsay, N. V. Len' and O. A. Vyviurska, *Micropor. Mesopor. Mater.*, 2013, **167**, 155-161; (c) H. H. Zhang and H. R. Li, *J. Mater. Chem.*, 2011, **21**, 13576-13580.
9. (a) P. P. Cao, Y. G. Wang, H. R. Li and X. Y. Yu, *J. Mater. Chem.*, 2011, **21**, 2709-2714; (b) Y. X. Ding, Y. G. Wang, H. R. Li, Z. Y. Duan, H. H. Zhang and Y. X. Zheng, *J. Mater. Chem.*, 2011, **21**, 14755-14759; (c) Y. J. Li, B. Yan and L. Wang, *Dalton. T.*, 2011, **40**, 6722-6731.
10. (a) S. Choi, R. M. Dickson and J. H. Yu, *Chem. Soc. Rev.*, 2012, **41**, 1867-1891; (b) A. V. Pokropivny and S. Volz, *J. Mater. Sci.*, 2013, **48**, 2953-2960; (c) C. Jensen, D. Buck, H. Dilger, M. Bauer, F. Phillip and E. Roduner, *Chem. Commun.*, 2013, **49**, 588-590.
11. (a) X. W. Cheng, Q. Y. Meng, J. Y. Chen and Y. C. Long, *Micropor. Mesopor. Mater.*, 2012, **153**, 198-203; (b) S. Ramachandra, Z. D. Popovic, K. C. Schuermann, F. Cucinotta, G. Calzaferri and L. De Cola, *Small*, 2011, **7**, 1488-1494; (c) H. Watanabe, K. Fujikata, Y. Oaki and H. Imai, *Chem. Commun.*, 2013, **49**, 8477-8479.
12. (a) G. Bellussi, A. Carati, C. Rizzo and R. Millini, *Catal. Sci. Technol.*, 2013, **3**, 833-857; (b) N. Lauridant, T. J. Daou, G. Arnold, H. Nouali, J. Patarin and D. Faye, *Micropor. Mesopor. Mater.*, 2013, **172**, 36-43; (c) X. G. Li, C. Liu, J. Sun, H. Xian, Y. S. Tan, Z. Jiang, A. Taguchi, M. Inoue, Y. Yoneyama, T. Abe and N. Tsubaki, *Sci. Rep-Uk.*, 2013, **3**.
13. (a) M. Watabe, R. Kuroda, M. Ushio, M. Ogasawara, S. Nakata and T. Haruyama, *J. Jpn. Petrol. Inst.*, 2012, **55**, 332-338; (b) J. Xie, Z. Wang, D. Y. Wu, Z. J. Zhang and H. N. Kong, *Ind. Eng. Chem. Res.*, 2013, **52**, 14890-14897; (c) D. Zhou, X. H. Lu, J. Xu, A. A. Yu, J. Y. Li, F. Deng and Q. H. Xia, *Chem. Mater.*, 2012, **24**, 4160-4165.
14. (a) H. S. Kim and K. B. Yoon, *J. Am. Chem. Soc.*, 2012, **134**, 2539-2542; (b) H. S. Kim, N. C. Jeong and K. B. Yoon, *J. Am. Chem. Soc.*, 2011, **133**, 1642-1645; (c) H. S. Kim, N. C. Jeong and K. B. Yoon, *Langmuir*, 2011, **27**, 14678-14688.
15. (a) H. S. Kim, C. T. P. Tung and K. B. Yoon, *Chem. Commun.*, 2012, **48**, 4659-4673; (b) T. Miyanaga, Y. Suzuki, N. Matsumoto, S. Narita, T. Ainaï and H. Hoshino, *Micropor. Mesopor. Mater.*, 2013, **168**, 213-220; (c) T. Yumura, T. Nanba, H. Torigoe, Y. Kuroda and H. Kobayashi, *Inorg. Chem.*, 2011, **50**, 6533-6542.
16. (a) E. Coutino-Gonzalez, M. B. J. Roeffaers, B. Dieu, G. De Cremer, S. Leyre, P. Hanselaer, W. Fyen, B. Sels and J. Hofkens, *J. Phys. Chem. C.*, 2013, **117**, 6998-7004; (b) H. T. Sun, Y. Sakka, N. Shirahata, Y. Matsushita, K. Deguchi and T. Shimizu, *J. Phys. Chem. C.*, 2013, **117**, 6399-6408.
17. (a) Y. J. Gu and B. Yan, *Eur. J. Inorg. Chem.*, 2013, 2963-2970; (b) B. Yan, *Rsc. Adv.*, 2012, **2**, 9304-9324; (c) B. Yan and Y. J. Gu, *Inorg. Chem. Commun.*, 2013, **34**, 75-78.
18. (a) H. Maas, A. Currao and G. Calzaferri, *Angew. Chem. Inter. Ed.*, 2002, **41**, 2495-2497; (b) S. T. Selvan, T. Hayakawa and M. Nogami, *J. Non-Cryst. Solids*, 2001, **291**, 137-141; (c) Y. Zhao and B. Yan, *Photochem. Photobio.*, 2012, **88**, 21-31.
19. (a) J. M. Kneller, T. Pietrass, K. C. Ott and A. Labouriau, *Micropor. Mesopor. Mater.*, 2003, **62**, 121-131; (b) H. S. Kim, N. C. Jeong and K. B. Yoon, *J. Am. Chem. Soc.*, 2011, **133**, 1642-1645; (c) Y. Ding, Y. Wang, H. Li, Z. Duan, H. Zhang and Y. Zheng, *J. Mater. Chem.*, 2011, **21**, 14755-14759.